 

# Gravity–driven flammable vapour clouds

Graham Atkinson, Health and Safety Executive, Harpur Hill, Buxton, U.K.

The majority of very large vapour cloud explosions occur in such low wind speeds that vapour flow is gravity-driven. Detrainment of heavy gas by the wind is so low that almost all of the gas released remains in a gas "blanket", which typically slumps in all directions around the source. Such gravity driven flammable clouds may extend many hundreds of metres from the source without significant dilution: their development cannot be assessed with conventional windy dispersion models.

Previous work on the basic problem of gravity-driven vapour transport on a flat open surface is reviewed. Existing methods suffer from a number of deficiencies including arbitrary specification of current height and velocity and the neglect of surface friction.

A new method of analysis is presented. Close to the source the flow can be calculated by forwards integration of mass and continuity equations. Entrainment of fresh air and friction increase the stability of the flow (Richardson number) and the rate of dilution declines towards zero. When the Richardson number approaches unity the current becomes critical and further out from the source the flow is under downstream control.

Predictions are compared with data from the Buncefield incident.

**Keywords**

Vapour cloud, gas cloud, axisymmetric, gravity-driven, entrainment, Richardson number, nil-wind dispersion. vapour cloud explosion.

## Introduction

A recent review of very large vapour cloud explosions (Atkinson and Hall, 2015, Atkinson et al., 2016) showed that more than 70% of those incidents occurred in such low wind speeds that vapour flow was gravity-driven. In these cases the rate of detrainment of heavy gas by the wind was so low that almost all of the gas released remained in a gas "blanket", which typically slumped in all directions around the source.

Figure 1 shows an example with this type of vapour transport (CSB, 2015). Overfilling of a gasoline tank in very still wind conditions led to the generation of a gravity-driven cloud that extended up to 500m from the source.

Figure 1: Burn pattern left by a gravity–driven vapour current – source marked by circle

Development of clouds like this is an important part of the risk profile at many flammable sites and may dominate the total off-site risk. For example, in the UK, land-use planning decisions near gasoline storage depots are made on the basis of gravity-driven vapour flow scenarios (HSE SPC/TECH/GEN). In this case the extent and concentration of fuel of the cloud are simply and directly based on experience in the Buncefield incident (Buncefield Major Incident Investigation Board, 2007).

## Existing methods of assessment

The scale and destructive power of this kind of incident means there is a pressing need for methods to assess the vapour transport that can account for site specific factors such as vapour production rate, surface roughness and topography.

A simple approach is described in FABIG Technical Note 12 (FABIG, 2013) which provides a means of calculating the source term (vapour volume production rate) for tank overfill incidents in calm conditions. Although the volume and concentration of a cloud can be predicted with some confidence using this method, the cloud depth and extent cannot. On the basis of experience at a number of incidents, the FABIG TN12 method recommends that assessments for fairly flat sites

should be made on the assumption that the cloud spreads symmetrically and has a constant depth of two metres. This cannot be generally true and there are records of gravity driven clouds with depths significantly above and below this level.

The process of accumulation of a gas blanket on flat ground is modelled in DEGADIS (Havens and Spicer, 1988). In principle this model can be applied to purely gravity-driven vapour transport, but it has almost always been applied to intermediate wind speeds where there is initially significant accumulation in a gas blanket, but this grows to a size where detrainment balances the input of gas from the source.

In DEGADIS it is assumed that the gas blanket has a uniform height H (at any given time) but this height varies as a function of time depending on the volume production rate and the progress of the front of the gravity current. The front velocity, $u_f$, is modelled by assuming the Richardson number, $Ri_f$, is constant at the front.

$$Ri_f = \frac{g'H}{u_f^2} = 0.76 \qquad \text{where g' is the relative density of the gas} \quad g' = g.\frac{\rho_{cloud} - \rho_{amb}}{\rho_{amb}}$$

Applying this frontal equation together with conservation of volume of the released gas allows the radius and height of the cloud to be calculated. Some typical results for a case where g' = 0.5 and the gas volume production rate Q = 200 $m^3/s$ are shown in Figure 2. The predicted cloud height falls steadily with time and the velocity close to the source is high – and continuously increases with time.

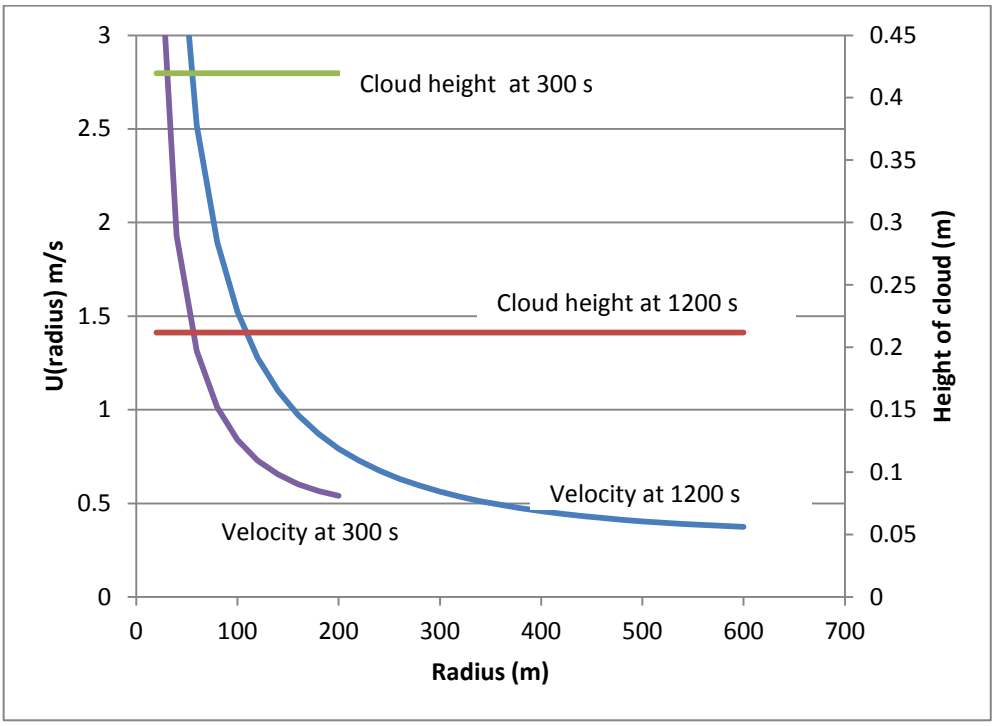


Figure 2: Cloud height and velocity calculated by the DEGADIS method

These cloud densities and volume production rates roughly correspond to conditions in the Buncefield incident – for which CCTV records provide data on the development of the cloud (Gant, 2006). The area around the tank did not correspond completely to the idealised flat open environment assumed in the model but, even allowing for this, there are some significant discrepancies between the model predictions and the observations. The model predicts a gradual decline in the cloud height with time and this is certainly not observed; on the contrary the height slowly increased. The predicted height close to the source is 0.4 m at t=300 s which is less than the observed height of >1m. The model predicts a gas velocity of around 3 m/s close to the source at 300 s; which is much larger than the observed velocity of <1m/s. However, the maximum extent of the cloud spread into flat areas was reasonably well predicted by DEGADIS; this is the key output when the code is used to determine the lateral size of a gas blanket that will act as a secondary source in a windy dispersion analysis.

The problem of axisymmetric spreading of a gravity current has been treated theoretically using a shallow water type model by Slim and Huppert, 2011. As in DEGADIS, their analysis used a Richardson number condition at the front, but with $Ri_f$ = 1.2. If entrainment of ambient fluid and friction are ignored, this work showed that the gas flows outward with approximately constant speed and with a cloud depth that decreases rapidly and continuously until close to the front, where there is a jump in height and rapid reduction in speed. These inviscid, non-entraining solutions are exact but do not correspond in a useful way to observations of the structure of vapour clouds during incidents. For example, it is predicted that, as time goes on, an ever-higher proportion of the total volume of gas released is concentrated in an area just behind the

front. This is not consistent with direct observations of the cloud, nor with the thermal and pressure damage caused during explosions.

Slim and Huppert went on to consider the effect of entrainment on cloud development. This greatly improved the potential usefulness of the solutions – reducing the thinning of the current and accumulation of gas behind the front. However their analysis neglected the effect of surface friction and the predicted vapour flows generally have relatively low Richardson numbers - below the limit at which significant entrainment dies away. Entrainment and dilution of the current continues until a point immediately behind the front. Without the inclusion of surface friction, the analysis does not predict the most important feature of a gravity current: the potential for gas to travel for distances of many hundreds of metres without significant dilution.

CFD offers the potential to account for the details of site topography – which is particularly important in gravity-driven vapour transport. A large number of studies have been carried out involving modelling of large scale tests in windy conditions (e.g. Gant et al. 2014). But there appear to be no large scale experimental data sets corresponding to continuous releases in near calm conditions - when vapour transport was dominated by gravity. A few studies have been carried out (Gant 2006, Venart and Rogers, 2011) in which CFD was used to analyse the vapour cloud development at Buncefield and other incidents in calm conditions. Comparisons in these gravity driven cases have focussed on the progress of the vapour front because this is generally the only quantitative data that is available. Unfortunately movement of the front is rather insensitive to the extent to which cloud structure and especially dilution are successfully modelled. Modelling of gravity driven flows over distances of many hundreds of metres is likely to be a significant challenge. Entrainments rates will be extremely low compared with windy dispersion analyses and additional issues of numerical diffusion are likely to arise. The first challenge is to demonstrate that a CFD code can in fact reproduce the long-range transport of vapour without significant dilution that the incident data indicate. Additional large scale tests, which could provide an opportunity for code validation, would be very valuable.

## New analysis

The method of calculation is summarised in Figure 3. Initially vapour flow is supercritical (Ri<1): this could be flow over a bund wall or slumping of a heavy, upwards facing jet. The development of the supercritical gravity current is controlled by the initial conditions, entrainment and friction. The method of calculation for this section of the flow simply involves forward integration of the momentum and continuity equations. The rate of entrainment and frictional stress can be assumed to be simple functions of the mean flow velocity.

The effect of entrainment and friction is to slow and deepen the gravity current and eventually the Richardson number rises to around 1. The flow becomes critical – any further increase in Richardson number would allow propagation of gravity waves upstream. These disturbances would rapidly reduce friction and any residual entrainment: and would tend to reverse the increase in Ri. In this way the flow progresses under downstream control with Ri about 1.

Near the front the flow is time dependent and again the Richardson number is of order 1.

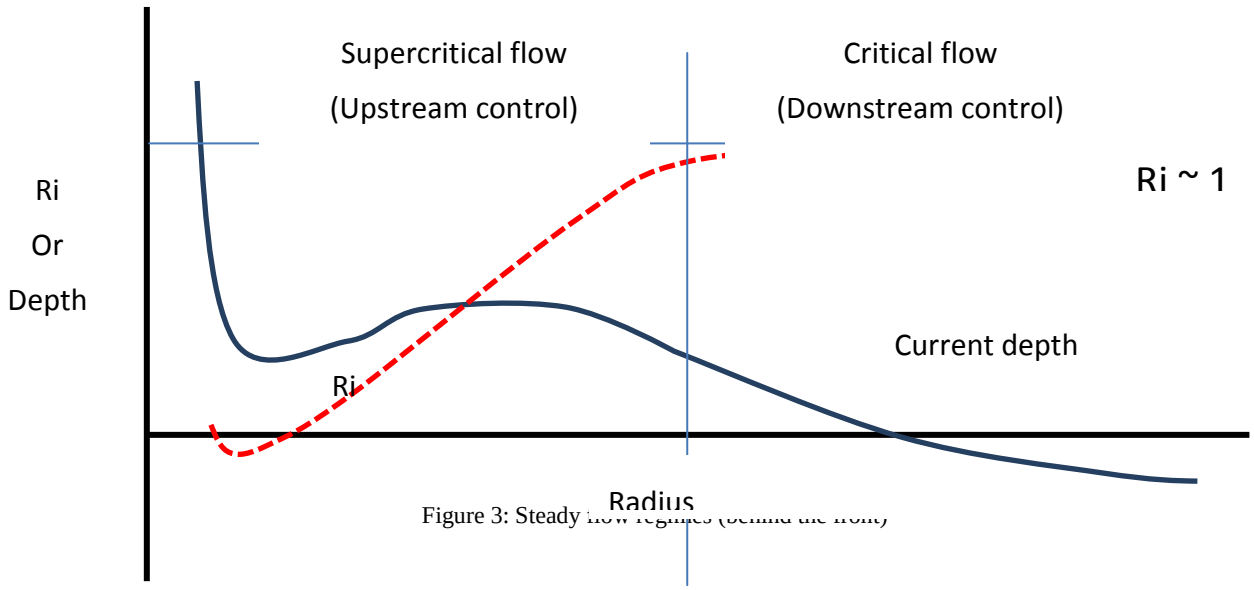


Figure 3: Steady flow regimes (behind the front)

### Supercritical flow close to the source

The basic mechanics of the supercritical current can be investigated by assuming constant values of velocity and concentration through the depth of the current – this is a similar approach to that taken by (for example) Slim and Huppert (2011) or Johnston and Hogg (2013). Well behind the front, the flow depth and velocity are constant (in time) which leads to

Continuity $$\frac{d}{dr}(UHr) = EUr \qquad [1]$$

where E is the ratio of entrainment velocity to flow speed , r is the radius and U the flow speed

Momentum $$\frac{d}{dr}(U^2 Hr) + r\frac{d}{dr}\frac{1}{2}g'H^2 = -u_*^2 r$$ [2]

$u_*$ is the shear velocity i.e. the surface shear stress is $\rho u_*^2$

Eliminating $\frac{dU}{dr}$ gives $$\frac{dH}{dr} = \frac{-\frac{H}{r} + k^2 + E\left(2 - \frac{Ri}{2}\right)}{1 - Ri} \quad \text{where } k = \frac{u_*}{U}$$ [3]

Also $$\frac{dRi}{dr} = -\frac{Ri}{r} + 3\frac{Ri}{H(1-Ri)}\left[-\frac{Ri.H}{r} + E\left(1 + \frac{Ri}{2}\right) + k^2\right]$$ [4]

These equations are easily integrated (e.g. with a spreadsheet) from a set of initial conditions. The dilution is calculated from H and Ri using the conservation of gas ( $g'UHr = const$ ) and the definition of Ri ($Ri = g'H/U^2$).

To begin with, additional air is entrained but, as the Richardson number rises, the rate of dilution decreases and eventually approaches zero. At this point the gas concentration in the wider cloud is fixed. Eventually the value of Ri approaches unity and the equations [3] and [4] become singular. The physical interpretation of this is covered in Section 5, where it is argued that further development of the current is under downstream control, with a Richardson number close to unity.

The low Ri limit of the equation for H is $\frac{dH}{dr} = -\frac{H}{r} + k^2 + 2E$

The maximum value of k is around 0.1 and the low Ri limit of E is around 0.08. This means that (for low Ri) changes in current depth are dominated by entrainment; friction has little effect. At large r and with $k^2 << E$ the solution of this equation is the familiar result for a conventional radial wall jet (minimal density variations).

H = Er

## Evaluating E at higher Richardson numbers

The value of the entrainment coefficient E is a function of Ri. Various relationships have been proposed for this function.

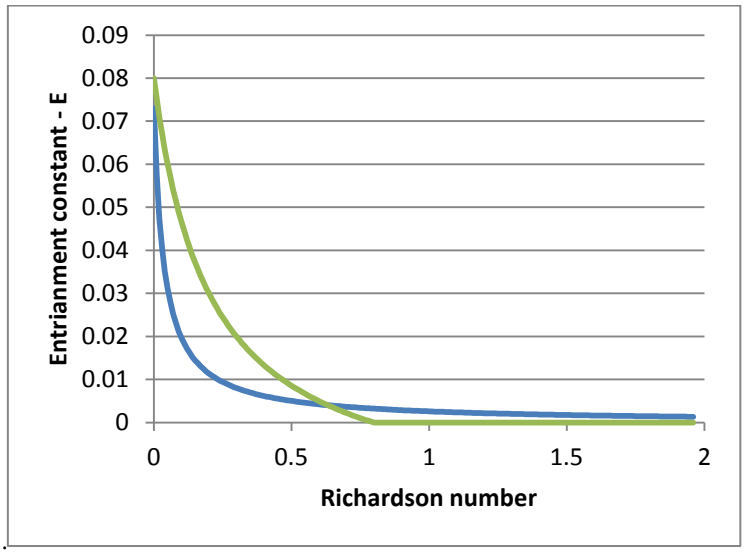


Figure 4: Entrainment constant as a function of Ri

*Green line – Slim and Huppert (2011) or Turner (1986)* $$E = \max\left[\frac{0.08 - 0.1Ri}{1 + 5Ri}, 0\right]$$ [5]

*Blue line – Johnson and Hogg (2013)* $$E = \frac{0.073}{1 + 27Ri}$$ [6]

These proposals vary significantly, but in both cases the rate of entrainment at Ri = 1 is very low or zero and friction may dominate any reduction in the thinning of the current.

It is worth noting that expressions like [6] with E proportional to 1/Ri for large Ri are used in many dispersion codes e.g. DEGADIS, PHAST (DNV, 2013). This appears to be largely based on measurements of entrainment by Lofquist (1960). Examination of the original data suggest that the small volume entrainment rates measured (nominally at high values of Ri) can be accounted for localised entrainment near the start of the current using the simple detrainment formula proposed by Briggs et al. (1990) for a deep fluid. Once a stably stratified interface is established the entrainment rates are probably extremely low and driven only by diffusion. For this reason the entrainment correlation shown in [5] is used in the supercritical analysis.

## Evaluating k ($u_*$/U)

The value of the friction velocity can be estimated from the roughness length for the surface $z_{rough}$ and cloud depth H. The roughness length is about 10% of the height of obstacles on the surface.

$$\frac{U}{u_*} = \frac{1}{\kappa}\ln\left(\frac{H}{z_{rough}}\right) \qquad \text{where } \kappa = 0.4 \text{ is von Karman's constant} \qquad [7]$$

Some values for H = 1 m and H = 2 m are shown below for a range of roughness lengths that would be appropriate for short (mown) grass (0.003) to moderately overgrown grass (0.03).

Table 1: Values of friction velocity $\frac{u_*}{U}$ as a function of roughness length and cloud depth

| | Cloud depth | |
|---|---|---|
| Roughness length (m) | 1m | 2m |
| 0.003 | 0.069 | 0.062 |
| 0.01 | 0.087 | 0.075 |
| 0.03 | 0.114 | 0.095 |

## Variation of cloud depth and velocity in a steady critical flow (Ri~1)

The element of the DEGADIS formulation that leads to discrepancies with observations is the arbitrary assumption that the cloud height is constant with radius. For circular symmetric spreading this leads to unrealistically high velocities close to the source. It is of interest to examine the consequence of different assumptions about the variation of cloud velocity and height with radius. We assume initially that only areas of the cloud quite close to the front are changing in time. This means that the quantity $r \cdot U(r) \cdot H(r)$ is constant with radius through most of the cloud. The appropriateness of this assumption has to be reviewed at the end of the analysis. If $U(r)$ is:

$$U(r) = U_0\left(\frac{R_0}{r}\right)^m \qquad \text{m is a (variable) index} \qquad [8]$$

Then $H(r)$ must vary as: $$H(r) = H_0\left(\frac{R_0}{r}\right)^{1-m} \qquad [9]$$

$R_0$ is the fixed radius at which the flow becomes critical. At large times it will be small compared with the frontal radius.

If the volume flow rate is Q, then the initial height, $H_0$, and velocity, $U_0$, (both at radius $R_0$) are related as:

$$Q = 2\pi \cdot R_0 \cdot H_0 \cdot U_0 \qquad [10]$$

Conservation of volume implies $$\int_{R_0}^{R_{\max}} H(r) \cdot 2\pi \cdot r \cdot dr = Qt \qquad [11]$$

Substituting $H(r) = H_0\left(\frac{R_0}{r}\right)^{1-m}$

Gives $$H_0 = \frac{(m+1)Qt}{2\pi R_0^{1-m} R_{\max}^{m+1}} \qquad R_{\max} >> R_0 \qquad [12]$$

A constant Ri condition at the front is appropriate.

$$\frac{dR_{\max}(t)}{dt} = C_E\sqrt{g\left(\frac{\rho-\rho_a}{\rho_a}\right)H(R_{\max},t)} \qquad \text{(with } C_E\sim 1\text{)} \qquad [13]$$

Values for the empirical constant $C_E$ vary from 0.91 (Slim and Huppert) to 1.15 (Havens and Spicer)

$$\frac{dR_{\max}(t)}{dt} = C_E\sqrt{\frac{g'(m+1).Q.t}{2\pi.R_{\max}^2}} \qquad [14]$$

This can be integrated to give to give (at large t):

$$R_{\max} = \sqrt{\frac{4}{3}}(m+1)^{\frac{1}{4}}\cdot C_E^{\frac{1}{2}}\cdot\left(\frac{g'}{2\pi}\right)^{\frac{1}{4}}\cdot Q^{\frac{1}{4}}\cdot t^{\frac{3}{4}} \qquad [15]$$

The time variation of $R_{\max}$ ($\propto t^{\frac{3}{4}}$) is independent of m and in line with experimental findings. This is why DEGADIS gives the correct functional dependence of the front location with time even though the assumptions about cloud depth are not correct.

In general $H_0$ and $U_0$ vary with time if $m \neq \frac{1}{3}$

$$H_0 \propto t^{\frac{1-3m}{4}} \qquad U_0 \propto t^{\frac{3m-1}{4}} \qquad [16]$$

The analysis was based on the assumption that cloud height close to the source does not vary with time – so that

$r\cdot U(r)\cdot H(r)$ is independent of radius. This is only consistent for $m = \frac{1}{3}$.

The Richardson number $Ri = \frac{g'H}{U^2}$ varies with radius if $m \neq \frac{1}{3}$ $\qquad Ri \propto r^{3m-1}$ [17]

For large times it is possible to express the cloud height and velocity in the simple time independent forms [1] and [2] only if

$$U(r) = U_0\left(\frac{R_0}{r}\right)^{\frac{1}{3}} \quad \text{and} \quad H(r) = H_0\left(\frac{R_0}{r}\right)^{\frac{2}{3}} \qquad [18]$$

In this case the Richardson number of the flow is uniform with radius. The front edge of the current advances as

$$R_{\max} = \left(\frac{4}{3}\right)^{\frac{3}{4}}\cdot C_E^{\frac{1}{2}}\cdot\left(\frac{g'}{2\pi}\right)^{\frac{1}{4}}\cdot Q^{\frac{1}{4}}\cdot t^{\frac{3}{4}} \qquad [19]$$

The expressions [18] allow the depth and velocity of the steady part of the current to be calculated from the radius and conditions when the flow becomes critical.

## Results of analysis

Examples illustrating the form of solutions to [3] and [4] for some example inputs are shown below. The Slim/Turner form of E(Ri) is used (Equation [5] and green curve in Figure 4 ).

### Example 1: Flow over a bund – roughly corresponding to the Buncefield case

The inputs in this example are shown below. Results are shown in Figure 5.

| | Initial values in Example 1 | | | | |
|---|---|---|---|---|---|
| k (friction) | Radius (m) | Vol. flow ($m^3/s$) | Depth (m) | g' ($m/s^2$) | Ri |
| 0.08 | 35 | 209 | 1 | 0.5 | 0.55 |

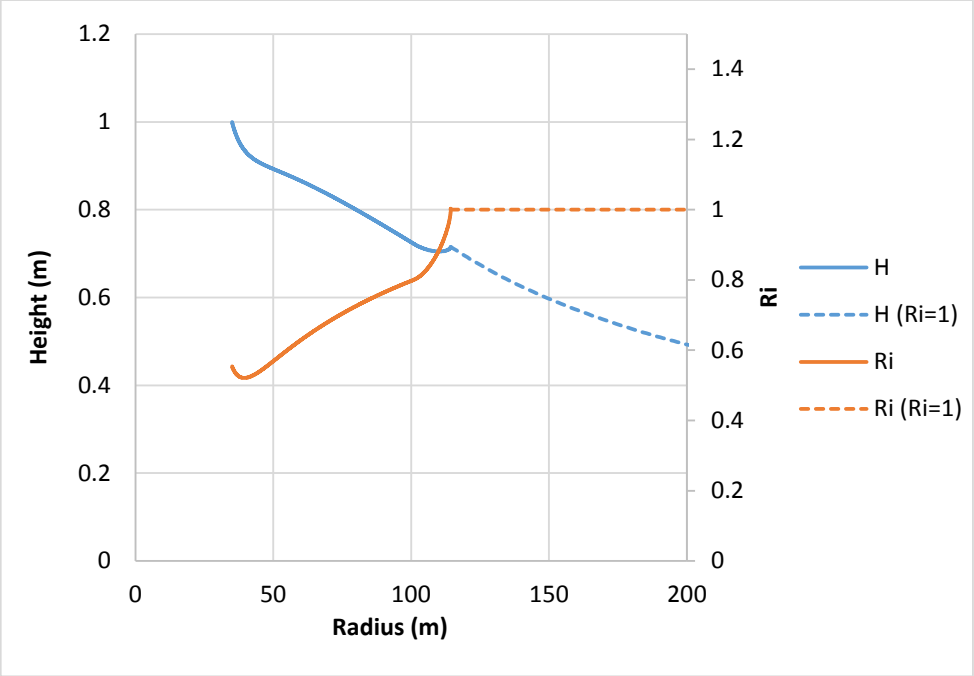


Figure 5a: Variation of gravity current height and Richardson number for Example 1

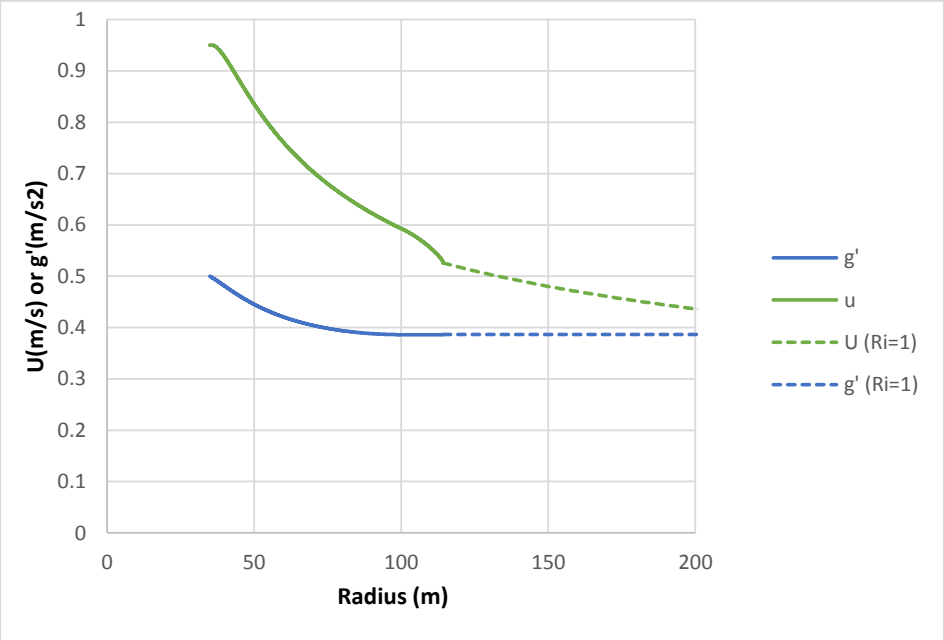


Figure 5b: Variation of gravity current velocity and concentration for Example 1

The Richardson number increases to 1 at a range of about 115 m. Overall the concentration in the current reduces to around 77% of its initial value before entrainment finishes. This flow could extend for very large distances with minimal entrainment (molecular diffusion is small and has been ignored). It is presumed that once the Richardson number reaches 1 it remains at this value and the flow varies according to [18].

### Example 2: Jet of LPG (vertically upwards)

In still conditions a vertical jet of LPG will eventually flow back to ground level around the source. In this case the source term radius may be much less and the initial vapour density difference (g') higher. A wide range of conditions may occur at the point where the gravity current returns to ground level – depending on the outlet pressure, degree of re-entrainment etc.

The example below uses typical values for low pressure jet rather than analysing any particular source.

| | Initial values in Example 2 | | | | |
|---|---|---|---|---|---|
| k (friction) | Radius (m) | Vol. flow ($m^3/s$) | Depth (m) | g' ($m/s^2$) | Ri |
| 0.08 | 5 | 209 | 1.8 | 2 | 0.26 |

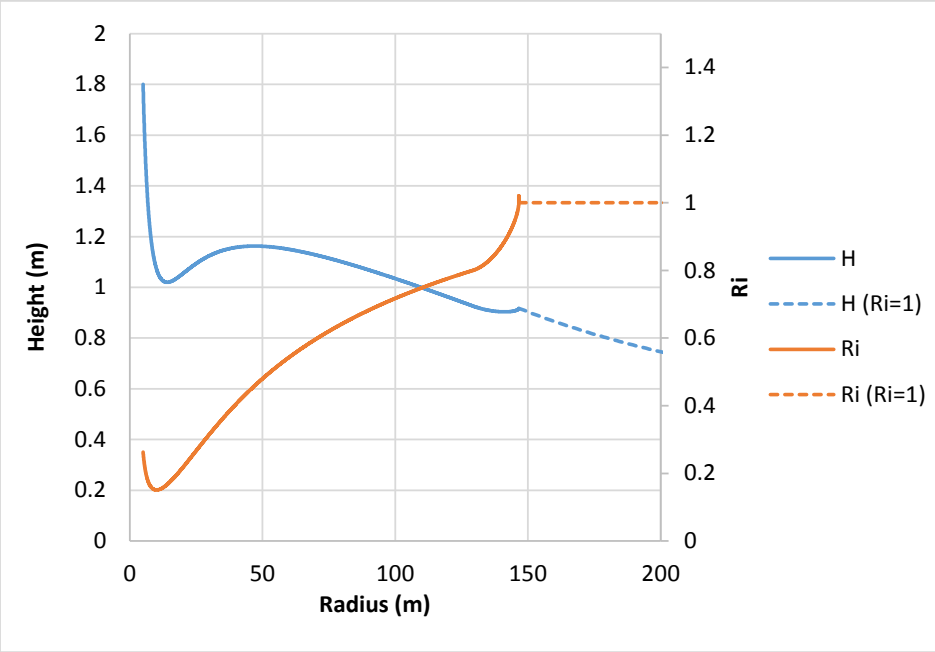


Figure 6a: Variation of gravity current height and Richardson number for Example 2

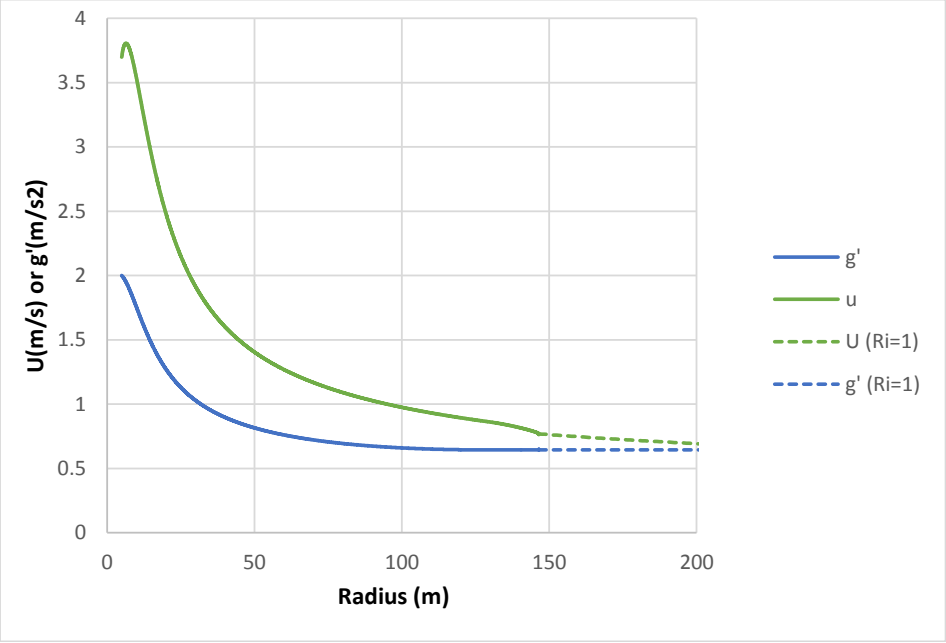


Figure 6b: Variation of gravity current velocity and concentration for Example 2

The Richardson number increases to 1 at a range of about 140 m. Overall the concentration in the current reduces to around 32% of its initial value before entrainment finishes. After this the flow could extend for very large distances with minimal entrainment. In this case the cloud at very long range would be flammable.

## Mechanics of a far-field constant Ri number flow

The simple time-independent forms for current depth and velocity in [18] are independent of the surface and roughness and any residual entrainment. This means they cannot be generally consistent with the lumped continuity and momentum equations [3] and [4] – which include entrainment and friction constants respectively. Instead such a constant Ri number flow would be controlled by the downstream boundary condition (at the front).

This apparent mismatch may be explained by considering the effects of a disturbance of the flow that results in a subcritical flow (Ri >1) at a given location. Such increase in Ri would corresponds to an increase in layer depth or a reduction in flow speed. For a subcritical flow (Ri>1) a time dependent change of this sort would produce a gravity wave that propagated back upstream. This wave would lead to both deepening and deceleration of the flow *upstream* of the original disturbance and associated variations in static pressure across the whole of the layer.

Friction and entrainment depend critically on the flow speed in a relatively thin boundary layer close to the lower and upper surfaces of the current respectively. These low speed flows are particularly sensitive to adverse pressure gradients: so a backward propagating gravity wave would produce relatively large proportional reductions in flow close to boundaries and consequently reductions in the frictional stress. In this way any increase in Ri above 1 would rapidly lead to a substantial reduction in upstream frictional stress and this would have the effect of strongly reducing Ri in the area where the original disturbance occurred. The effects of temporary disturbances taking Ri above unity would therefore tend to die away with time. A disturbance that took Ri below unity in a particular location would leave a supercritical flow. Friction or entrainment would tend to increase the Ri number towards 1 and such a disturbance would also tend to die away downstream.

The lumped momentum equation [4] is appropriate where there is a relatively fixed relationship between the surface friction and the velocity in the main current. This is a reasonable approximation for low Ri flows (Turner, 1973 and 1986) but is not appropriate in critical or sub-critical flows where propagation of gravity waves upstream can have a relatively large effect on boundary layer flow and surface friction.

Several authors have provided helpful descriptions of the flow structure within established non-entraining two-dimensional gravity currents (e.g. Thorpe, 1993, and Hallworth et al., 1996). The main flow of undiluted heavy fluid is separated from ambient air by a mixing layer extending to about 30% of the total depth, so the gradient Richardson number in this layer is around 0.3. Briggs et al (1990) use this finding to derive important estimates of the total amount of entrainment required to establish the stable flow.

For an axisymmetric current it is, at first sight, hard to see how such a structure could be maintained over a long distance. Geometric factors lead to a thinning of the current and this would require an adjustment of the depth of the mixing layer (and potentially additional entrainment ) unless the speed of the current simultaneously reduces to maintain stability. Only friction can drive such a reduction in speed and the shear needs to produce just the right degree of slowing of the flow *whatever the nature of the surface.* In fact the stable flow structure can be maintained if the Richardson number of the layer is constant and the arguments above describe how this may occur in a way that does not depend on the roughness of the surface.

## Comparison with incident data from Buncefield

Gant reports CCTV data on the early progress of the vapour cloud across a flat, open area to the west of the source (Gant 2006). Six minutes after over-topping the bund, vapour was observed in a thin layer up to 200 m from the source (Figure 7).

Figure 8 shows a comparison between CFD, observations and [19] with $C_E$ = 0.91 and $C_E$ = 1.15 corresponding to the range of uncertainty in this parameter. The correspondence is within the uncertainly associated with the data and [19] probably provides a reasonable estimate of cloud spread in very flat, unobstructed conditions. The observed cloud depth is not easy to judge in Figure 8 but it appears to roughly correspond to the results in Figure 5a, i.e. a depth of around 0.5 m at a range of 200 m.

Later on the progress of the vapour cloud at Buncefield was strongly constrained by gradients around the site and the blocking effect of large buildings.

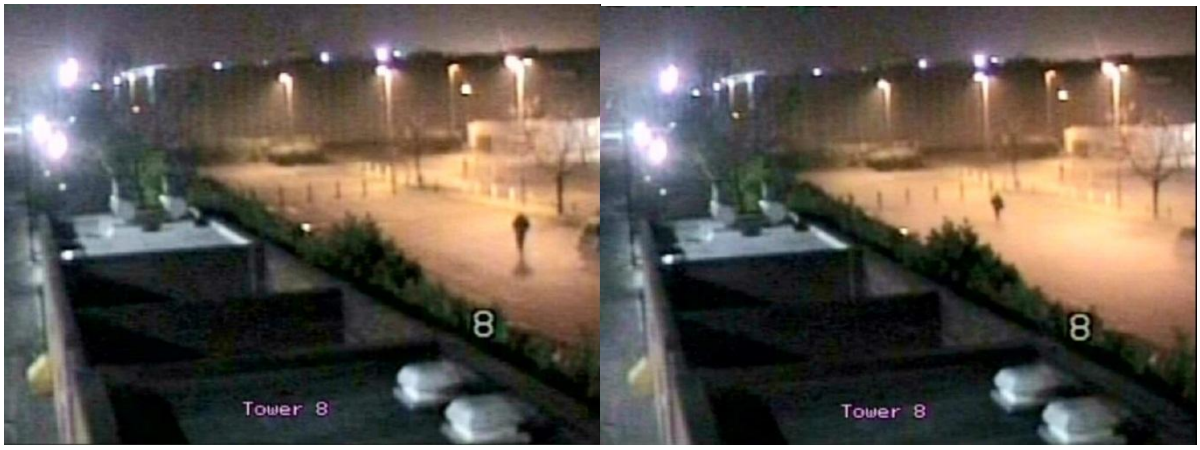


Figure 7: Before and after arrival of the low lying vapour current in an area around 200 m from the source.

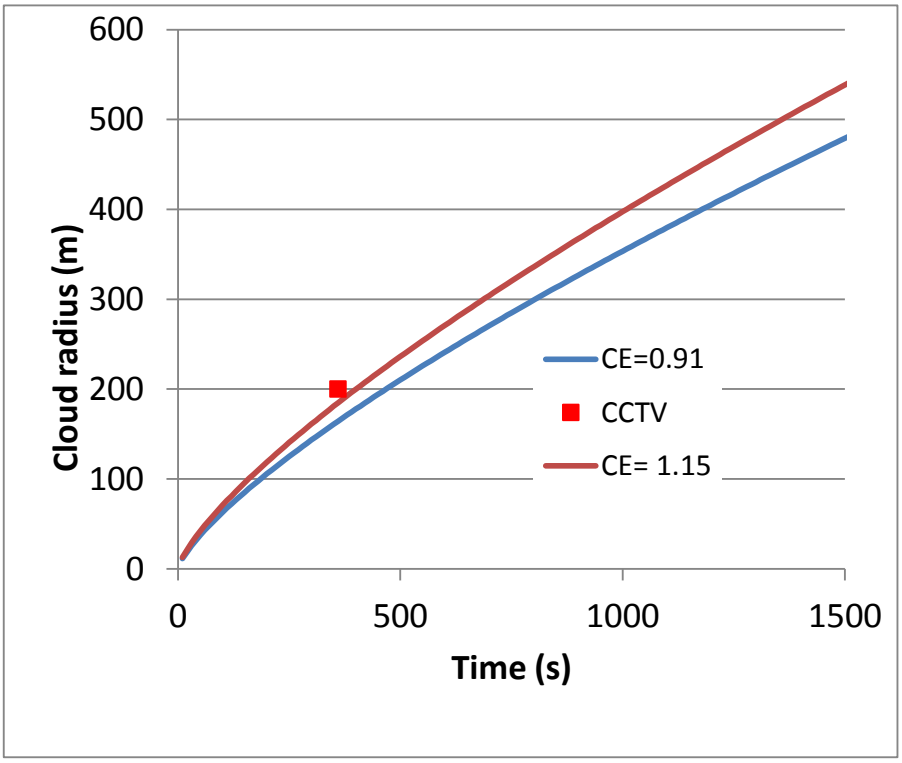


Figure 8: A comparison between observed and predicted cloud spread across a flat, open part of the Buncefield site

## Discussion

This work provides a quantitative explanation for the observation, that in calm conditions, vapour clouds can travel very large distances on flat ground without high levels of dilution. If there is constraint on the gravity-driven flow in the far-field e.g. upward slopes or walls or perhaps dense high vegetation, then the flow will back-up, producing a deeper layer, again without significant dilution.

Many sites will not conform to the ideal of flat unobstructed flow analysed here. In this case [19] will over-predict the likely reach of a cloud and under-predict its depth. The recommendations in FABIG Technical Note 12 may be a better general guide to cloud size in this case.

CFD provides a means of allowing for site topography and this could be a useful means of assessing the area that might be affected by a cloud. This prediction is reasonably insensitive to the level of entrainment. CFD solutions that indicate rapid dilution of the vapour current below the flammable limit should be examined carefully for the effects of numerical diffusion.

## Disclaimer

This paper and the work it describes were funded by the UK Health and Safety Executive (HSE). Its contents, including any opinions and/or conclusions expressed, are those of the author alone and do not necessarily reflect HSE policy.

## References

Atkinson, G. and Hall, J. (2015) A review of large vapour cloud incidents, HSL Report MH15/80 http://primis.phmsa.dot.gov/meetings/MtgHome.mtg?mtg=111

Atkinson,G., Cowpe, E., Halliday, J. and Painter, D., (2016) *A Review of Very Large Vapour Cloud Explosions*. 19th Mary Kay O'Connor International Process Safety Symposium, College Station TX October 2016.

Briggs, G.A., Thompson, R.S. and Snyder, W.H., (1990), *Dense gas removal from a valley by crosswinds*, J. Haz. Mat., Vol **24**, p.1-38.

Buncefield Major Incident Investigation Board (2007) *The Buncefield Incident – 11th December 2005 – The Final Report of the Major Incident Investigation Board, Vol. 1*., ISBN 978-07176-6270-8. http://www.hse.gov.uk/comah/buncefield/miib-final-volume1.pdf

CSB US. Chemical Safety and Hazard Investigation Board, (2015), *Caribbean Petroleum Tank Terminal Explosion and Multiple Tank Fires (October 23rd 2009) – Final Investigation Report.*

DNV (2013) Phast Version 7 Software, DNV Software, London, UK. Available from http://www.dnv.com/software, accessed 19 August 2013.

FABIG (2013) *FABIG Technical Note 12 - Vapour cloud development in over-filling incidents*, April 2013. Available from http://fabig.com/video-publications/TechnicalGuidance#,

Gant, S., (2006), *Buncefield Investigation: Dispersion of the Vapour Cloud*, HSL Report CM/06/13.

Gant, S.E., Narasimhamurthy, V.D., Skjold, T., Jamois, D. and Proust, C. (2014) *Evaluation of multi-phase atmospheric dispersion models for application to Carbon Capture and Storage*, Journal of Loss Prevention in the Process Industries, Volume 32, November 2014, Pages 286–298

Hallworth, M.A., Huppert, H.E., Phillips, J.C. and Sparks, R.S.J. (1996) "Entrainment into two-dimensional and axisymmetric turbulent gravity currents", ***J. Fluid Mech.*** **308**, 289-311.

Havens, J. and Spicer, T.,(1988) "A dispersion model for elevated dense gas jet chemical releases", EPA Report EPA-450/4-88-006a.

HSE SPC /TECH/GEN 43 Land use planning advice around large scale petrol storage sites http://www.hse.gov.uk/foi/internalops/hid_circs/technical_general/spc_tech_gen_43/

Johnson, C.G. and Hogg, A. J. (2013), *Entraining gravity currents*, J.Fluid Mech., Vol **731**, p471-508

Lofquist, K. (1960), *Flow and Stress Near an Interface between Stratified Liquids*, Phys. Fluids Vol 3, p.158-175.

Poreh, M., Tsuei, Y. G. and Cermak, J. E. (1967) *Investigation of a Turbulent Radial Wall Jet*, J. Appl. Mech 34(2), p457-463.

Slim, A.C. and Huppert, H.E., (2011), *Axisymmetric , constantly supplied gravity currents at high Reynolds number*, Journal of Fluid Mechanics volume 675, pp 540-551.

Thorpe, S.A., (1973), *Experiments on instability and turbulence in a stratified shear flow*, J. Fluid Mech., 61, p.731-751.

Turner, J. (1973), *Buoyancy effects in fluids*, Cambridge University Press.

Turner, J. (1986), *Turbulent entrainment: the development of the entrainment assumption, and its application to geophysical flows*, Journal of Fluid Mechanics, Vol. 173, p.431-47.

Venart, J. E. S. and Rogers, R. J., (2011) *The Buncefield explosion: vapour cloud dispersion and other observation*, Hazards XXII, IChemE Symposium Series No. 156.